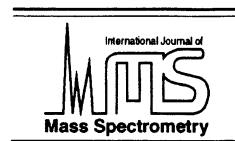




ELSEVIER

International Journal of Mass Spectrometry 192 (1999) 87–97



# Electron cyclotron resonance ion sources of highly charged ions: from classical to superconducting sources

G. Melin

*Département de Recherche Fondamentale sur la Matière Condensée Service des Ions, des Atomes et des Agrégats, CEA/Grenoble 17 rue des Martyrs, 38054, Grenoble Cédex 9, France*

Received 31 May 1999; accepted 10 June 1999

---

## Abstract

Along their continuous performance progression, electron cyclotron resonance ion sources (ECRIS) of highly charged ions must now cope with new demanding confinement requirements, specifically, higher magnetic fields in devices of larger dimensions, that can be realized only with superconducting coils. In this article we deal with the present state of the art of ECRIS, summarize the underlying plasma physics and the main ECRIS issues, and present the source performances and the existing and projected devices. Emphasis is given to the expected perspectives of the transition from present “classical” sources (those using only copper coils and permanent magnets) to superconducting sources using superconducting windings. (Int J Mass Spectrom 192 (1999) 87–97) © 1999 Elsevier Science B.V.

*Keywords:* Electron cyclotron resonance; Ion sources; Highly charged ions; Superconduction

---

## 1. Introduction

Despite their progression in performances, the electron cyclotron resonance ion sources (ECRIS) are now facing new requirements in order to produce ion beams either of higher charge states or of higher intensities. In this article we consider the present evolution of “classical” sources, i.e. the sources now in operation, and those basically using only copper coils and/or permanent magnets [1,2]. These classical ECRIS, although they are of high performance and now universally operate in most accelerator facilities as well as in small scale experiments, are subject to the well-known limiting effects of high charge state production and ion current saturation. Fig. 1 illustrates

the latter effect: as a function of the input rf power the production of any multiply charged ion necessarily saturates. For reasons that will be developed in the next section, sources with higher magnetic fields operating at higher frequencies were built in order to beat back these limitations. Therefore modern ECRIS are now approaching the domain of multiteslas magnetic fields that can be produced only by superconducting windings. Moreover this obeys the imperious necessity of having large ECRIS plasmas in order to produce very highly charged ions, and eventually large intensities as well.

## 2. Summary of ECRIS theory and main ECRIS issues

ECRIS are small mirror machines [1,2] equipped with a radial minimum-B magnetic multipole, usually

---

E-mail: gmelin@cea.fr

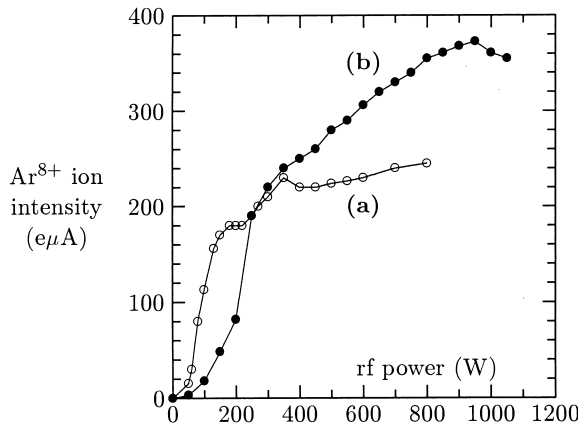


Fig. 1. Saturation of the extracted  $\text{Ar}^{8+}$  ion intensity as a function of the input rf power from a 14 GHz Caprice source for different tuning conditions: ion intensity initially optimized at (a) 100 W, (b) 500 W prior to rf power excursion.

hexapolar and made of permanent magnets. In such a magnetic configuration the equal- $|B|$  surfaces are closed and nested inside each other with  $|B|$  increasing outwards (Fig. 2). The electrons are heated by interacting with a rf wave at cyclotron resonance when crossing the closed equal- $|B|_{\text{ecr}}$  surface, where the electron Larmor frequency is equal to the wave frequency. Basically an ECRIS confines a hot electron plasma; its main components are: (1) the magnetic configuration, i.e. the plasma container, (2) the rf

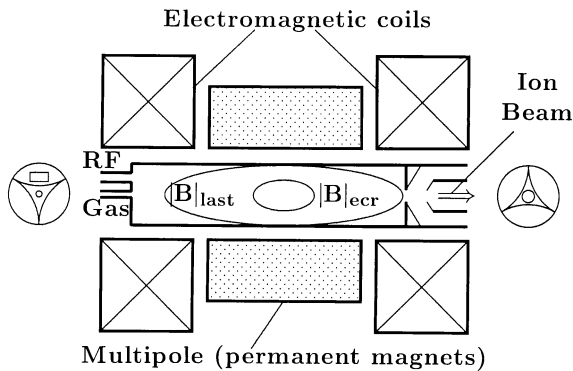


Fig. 2. Sketch of an ECR ion source of multicharged ions:  $|B|_{\text{ecr}}$  refers to the closed electron cyclotron resonance surface,  $|B|_{\text{last}}$  refers to the highest closed  $|B|$  surface of electron confinement. The prints left by the plasma (magnetic field lines) on the end plates within the plasma chamber are shown at injection and at extraction.

power input, i.e. the source of energy that heats up and sustains the plasma electrons in the magnetic trap, (3) the internal (ionization) and external sources of electrons, which allow the electron density to build up, and (4) the injected neutrals (gas or metal), i.e. the fuel injected in order to compensate for the ion losses and to control the neutral pressure. The extracted ion currents at one end of the device are actually the ion losses of the trapped plasma, therefore the ion current  $I_i^q$  of species  $i$  and charge state  $q$  is given by an expression of the form

$$I_i^q \approx \frac{1}{2} \frac{n_i^q q e V_{\text{ex}}}{\tau_i^q} \quad (1)$$

where  $n_i^q$  is the density of ions of species  $i$  and charge state  $q$ ,  $\tau_i^q$  the ion confinement time, and  $V_{\text{ex}}$  is the part of the hot plasma volume that maps along the magnetic field lines into the extraction area. The hot plasma volume is actually that of the closed equal- $|B|_{\text{ecr}}$  surface. Because of plasma charge neutrality one may expect the higher  $n_e$  the electron density, the larger the extracted ion current  $I_i^q$  of a given charge state.

## 2.1. Electrons

Theoretical [3] and experimental [4] works on electrons of ECRIS plasmas show that the electron velocity distribution function is not Maxwellian, although it can be schematically represented by several Maxwellian distributions: cold, warm, and hot. However electrons, although not Maxwellian, may be abusively described by a single Maxwellian distribution—that of hot electrons which carry (by far) almost all the electron energy with respect to cold and warm electrons. The efficiency of the electron confinement that determines to some extent both the density  $n_e$  and “temperature”  $T_e$  of electrons, strongly depends upon the mirror ratio  $R$ . Here  $R$  is defined as the ratio of the maximum magnetic field encountered by the electrons while they move within the plasma chamber without touching the walls to the resonance magnetic field,

$$R = \frac{B_{\text{last}}}{B_{\text{ecr}}} \quad (2)$$

$B_{\text{last}}$  corresponds to the  $|B|$  surface of the magnetic configuration that is fully within the plasma chamber and hardly touches the walls (Fig. 2),  $B_{\text{ecr}} = m_e \omega_{\text{rf}} / e$  is the cyclotron resonance magnetic field. The larger the mirror ratio, the better the quality of the magnetic configuration, or equivalently the smaller the so-called mirror loss cone, i.e. the electron velocity space zone where electrons are not confined [1,2].

The quality of the magnetic trap should be enough in itself to allow for the confinement of a given plasma (product  $n_e T_e$ ), although Coulomb collisions of electrons with other particles, both electrons and ions, would reduce the increase of the plasma parameters  $n_e$  and  $T_e$  as a function of the input rf power. Experimentally, however, as the rf power increases, the electron density first increases, then saturates, and eventually drops. This is also the case for the extracted ion currents (Fig. 1). Obviously such phenomena cannot be accounted for only by Coulomb collisions: increasing the rf input power does not necessarily lead to a higher electron density, and the rf input power may not be absorbed as well. Theory [3] has given a coherent explanation: the rf wave magnetic field induces supplementary electron losses with respect to collisional losses. This effect becomes important when the rf wave phase velocity in the ECR plasma, which normally decreases as the electron density increases, approaches the electron velocity. An ultimate limit for the product  $n_e T_e$  of the ECR plasma parameters (if it were really Maxwellian) can be theoretically found [3] as,

$$(n_e T_e)_{\text{max}} \approx \frac{(m_e \epsilon_0 \omega_{\text{rf}}^2)}{e^2} m_e c^2 \quad (3)$$

The first fraction is actually equal to the plasma electron density (more commonly called cutoff density) for the frequency  $\omega_{\text{rf}}$ . The important thing is the higher the frequency the larger the possible product  $n_e T_e$ . This explains why working at higher rf frequency in ECRIS, and therefore at high magnetic fields while keeping a high mirror ratio, is an important ECRIS issue with regard to both high charge state

ion production and high ion beam intensities, from the perspective of electron confinement. However there are also conditions more specifically related to ion confinement.

## 2.2. Ions

The behavior of highly charged ions in ECRIS is somewhat strange. Although electrons are energetic, ions are rather cold. Owing to the large ratio of ion to electron masses and to the large average electron energy, the electron–ion collisional heating cannot be very efficient and the electron–ion energy equipartition occurs on a timescale (in the range of a few seconds) much longer than that of the ion confinement—about three orders of magnitude [5]! The ion–ion collision frequency is large enough so that the energy equipartition terms between ions rapidly become negligible. Ions are therefore Maxwellian with the same temperature  $T_i$ , regardless of ion charge states or ion species. The ion temperature  $T_i$  is usually of the order of a few eV only. Although formula (1) would apparently give lower ion currents for larger ion confinement times, increasing the ion confinement time  $\tau_i^q$  will self-consistently increase the ion density  $n_i^q$  and the corresponding ion current  $I_i^q$ . As explained above, improving the electron confinement increases the electron density, which in turn decreases the ionization times. It can be shown [5] that the most abundant current delivered by an ECRIS, i.e. the peak of its charge state distribution (in currents), corresponds to the charge state for which ion confinement time and time of production of ions (this time strongly depends upon the ionization time) are close to each other. Therefore the improvement of ECRIS performances, both ion intensities and ion charge states, relies not only on electron confinement but also on ion confinement.

In high performance ECRIS, ions are highly collisional. Table 1 gives a few ion parameters (for argon ions of charge  $q = 10$ ) in a 14 GHz ECRIS. Because of their high collisionality ions are almost unmagnetized, with their mean free path  $\lambda$  being much shorter than their Larmor radius  $\rho_i$ ,  $\lambda / 2\pi\rho_i \ll 1$ . While moving within the plasma, they experience a random

Table 1  
Typical Ar<sup>10+</sup> ion parameters

$\nu_{ii}(\text{s}^{-1})$	$\nu_{ee}(\text{s}^{-1})$	$\tau_i^{10}(\text{ms})$	$f_{ci}(\text{s}^{-1})$	$\rho_i(\text{mm})$	$\lambda(\text{mm})$
$43.10^6$	0.28	a few ms	$1.5 \cdot 10^6$	0.16	0.04

walk diffusion essentially governed by collisions as illustrated in Fig. 3. While being confined, i.e. during the time  $\tau_i^q$ , an ion moves over the characteristic plasma dimension  $\ell$ , and undergoes  $N(=\tau_i^q \nu_{ij})$  collisions ( $\nu_{ij}$  being the ion–ion collision frequency), therefore statistically  $\ell \approx \sqrt{N} \lambda$  which leads to the following formula for  $\tau_i^q$  in the units s, cm, eV, cm<sup>-3</sup>

$$\tau_i^q \approx 7.1 \cdot 10^{-20} \ell^2 \ln \Lambda_{ij} \frac{q^2}{T_i^{5/2}} \sum_j \sqrt{A_j} \sum_q n_j^q q^2 \quad (4)$$

In this formula the Coulomb logarithm  $\ln \Lambda_{ij}$  is almost a constant ( $\approx 15$ ), the  $j$  summation is over all ions,  $A_j$  being the  $j$ th ion atomic mass number. Although there is still some controversy in the ion charge dependence of the ion confinement time [5], which may not be quadratic but only linear, as suggested by some experimental measurements [6], the formula (4) which is only statistically established, shows the importance of the parameter  $\ell$  and of the ion temperature. However, in current ECRIS [7] the

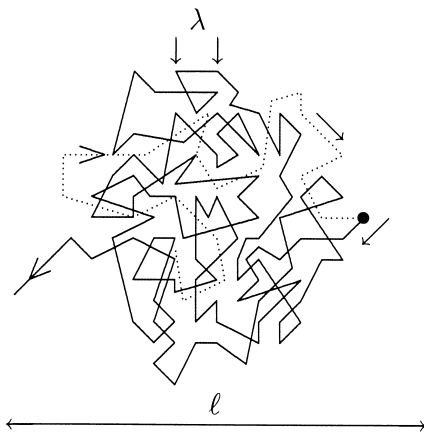


Fig. 3. Illustration of the random walk diffusion of a highly charged ion in ECRIS plasma.

characteristic plasma dimension  $\ell$  is given by the size of the ECR surface and the plasma chamber; it is only a few centimeters long ( $\leq 5$  cm). Increasing  $\ell$  would lead to an increase in the multipole diameter. This would conversely reduce the radial magnetic field usually created by permanent magnets, and therefore the source performance! Superconducting multipole windings would clearly offer the only opportunity to increase the source dimensions, and thus the ion confinement times and the extracted intensities as well.

### 3. Status of classical ECRIS

Amazingly, ECRIS development was often carried out in an empirical manner. The importance of the closed  $|B|$  surfaces of the magnetic configuration was experimentally discovered [1]. The importance of the mirror ratio  $R$  was also experimentally found [8]. Now high performance ECRIS have magnetic configurations with  $R$  as large as possible, usually  $R \approx 2$ . Aside from the magnetic configuration the increases of ECRIS performances were generally obtained by using either special developments sometimes assimilated to “tricks” or new experimental methods often called “recipes.” The underlying theoretical concepts associated with these tricks and recipes are not fully explained. Below are some of the most common recipes and tricks still currently applied by ECRIS users briefly analyzed: gas mixing, electron sources and other electron confinement improvement systems, afterglow effect, and double frequency operation. Other experimental methods would deserve more attention and development. For instance, a lot of efforts is still necessary in the field of rf heating and rf coupling systems.

#### 3.1. Gas mixing

This remarkable effect apparently consists of mixing a lighter gas with the main element of the ECR discharge in order to increase the output currents of highly charged ions of that element. By playing with the pressures—and therefore amounts—of both ele-

ments (added gas and main element) and the rf input power as well, it is possible to optimize the production of highly charged ions of the main element. The amount of gas being added is usually important with respect to that of the main element, and its mass is generally lower. Actually the gas mixing technique is related to an ion temperature reduction, or ion cooling, that improves the confinement times of highly charged ions, e.g. as shown in formula (4). Several mechanisms have to be accounted for in the gas mixing technique [5]: (1) the high losses of the added gas ions. Ideally, the added gas, e.g. oxygen, has only low charge states that have low confinement times as compared to those of the main element, e.g. argon, of which high charge state ion densities (and thus loss rates) have to be increased. Ion cooling is induced from enhanced ion energy losses after dilution. This refers to the importance of low charge states in gas mixing. (2) The mass effect of the added gas. Ideally the added gas mass is as close to that of the main element as possible, so as not to increase the ion energy from electrons, and to allow for easy exchange of energy with main element ions. This refers to minimizing the energy equipartition between electrons and ions, and to the strong coupling by collisions between all ions. It is important to point out that the added gas element mass is not lighter than that of the main element, as often mentioned. (3) However, practicing the gas mixing technique may reduce the plasma electron density and therefore all the ion densities, because of the lower ionization rates of the added gas with respect to those of the main element.

There are contradictions between these three criteria, and the optimization of high charge states by gas mixing results in a compromise. Fig. 4 shows the effect of gas mixing while optimizing the production of  $\text{Ar}^{14+}$  ions [5]. Data with no added gas, with oxygen 16, oxygen 18, and neon 22 as added gases are presented at different rf input power. The calculated ion temperature  $T_i$  of the corresponding plasmas is also presented. These data illustrate the compromise that leads to using oxygen 18 as the best added gas for that particular experiment.

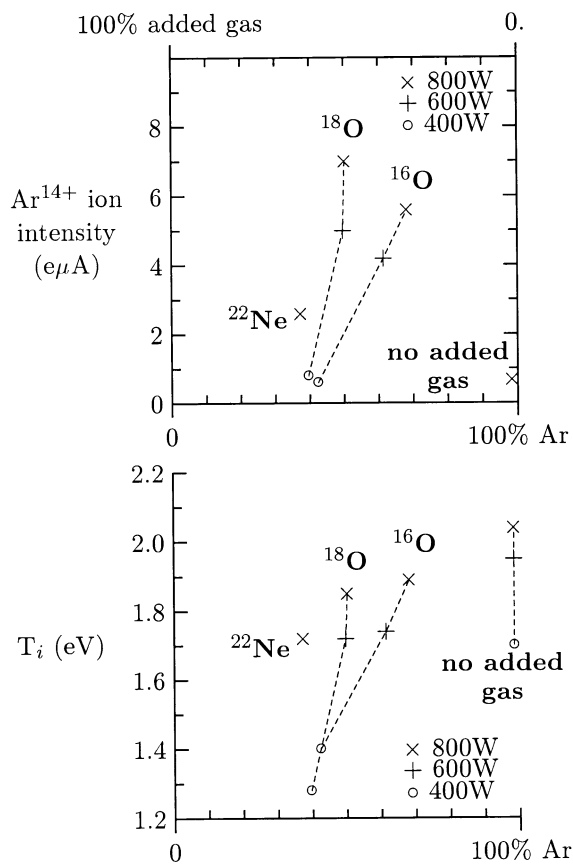


Fig. 4. Optimization of  $\text{Ar}^{14+}$  ion intensity with gas mixing in a Caprice source: top figure gives the optimized ion intensity for different gases (mass effect); bottom figure correspondingly gives the calculated ion temperature (ion cooling effect). The horizontal coordinate is the calculated Ar ions proportion in the plasma for the same data.

### 3.2. Electron sources

Both external electron sources that can supply electrons to the ECRIS plasma, and other external systems as well that can reduce the electron losses, efficiently boost the total electron density and the ECRIS performances. A lot of work has been achieved on electron sources, first stage, plasma cathode, and electron gun [1,2]. Electron donors such as coatings ( $\text{Al}_2\text{O}_3$ ) on the plasma chamber walls (sometimes made of aluminum) are also very often used for high charge state ion production [7,9]. In the category of systems reducing the electron losses,

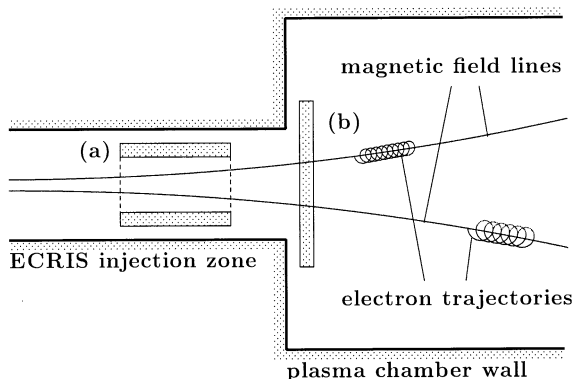


Fig. 5. Examples of biased electrodes in ECRIS injection zone: (a) cylinder, (b) disc.

negatively biased electrodes as shown in Fig. 5 are now frequently utilized. By varying the applied voltage they can operate in a broad range of parameters and ion species; however, it is not clear whether a biased electrode improves the cold electron confinement or provides more electrons from the secondary emission of impinging plasma particles.

### 3.3. Afterglow effect

This is another remarkable ECRIS effect that is shown in Fig. 6. When turning the rf power off, it is possible to observe a rapid increase in the delivered intensity of highly charged ions. This effect is interpreted as a consequence of the non-Maxwellian elec-

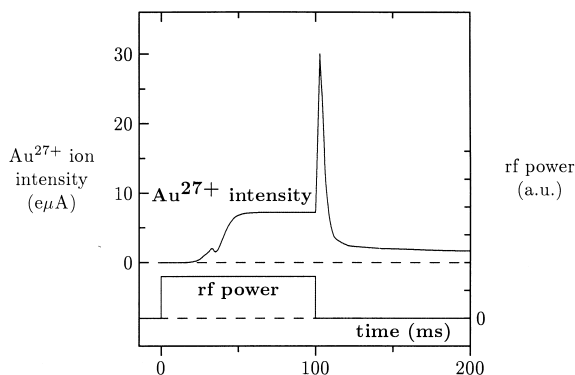


Fig. 6. Example of afterglow pulse obtained on  $\text{Au}^{27+}$  ion current at rf power turn-off.

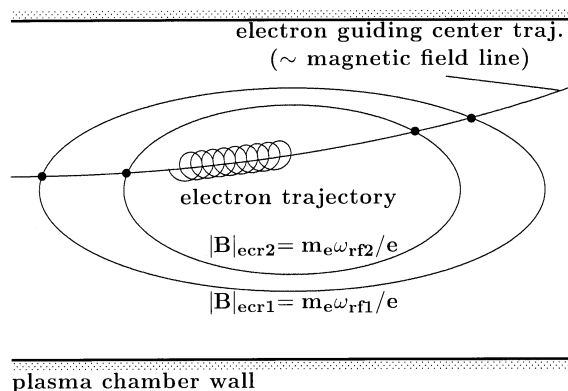


Fig. 7. The principle of the double frequency operation, the black dots indicate the resonance zones where electrons receive energy from the input rf powers.

tron velocity distribution in steady state. At the rf turn-off cold electrons that are not rf-heated anymore leave the plasma faster than the hot ones, therefore the charge balance of the plasma induces enhanced ion charge losses accordingly. ECRIS currently operate in this pulsed mode to supply lead beams of intensity as large as  $120 \text{ e}\mu\text{A}$  of  $\text{Pb}^{27+}$  [10]. It is expected that this functioning mode of interest for synchrotrons be able to deliver intense pulses of highly charged ions, a few mA and a few ms, in future ECRIS.

### 3.4. Double frequency operation

This mode of operation for ECRIS was successfully developed on the Berkeley AECR ion source [11]. It basically consists of simultaneously using two heating frequencies; most of the rf power is usually injected at the higher frequency,  $\omega_{rf1}$ , whereas a small amount of additional power is injected at the lower frequency,  $\omega_{rf2}$ . The most commonly admitted functioning of the double frequency operation is illustrated in Fig. 7. The electron confinement—and the source performance—would get improved by the synergistic effect of both frequencies. The electrons moving back and forth along the magnetic field lines (Fig. 7) receive kicks of transverse energy when crossing the resonance zones. The additional resonance zones that are created by the second frequency could secure more electrons from being lost. Equivalently, the additional

Table 2

Parameters of operative ECRIS: axial field at injection (wall)  $B_{\text{inj}}^w$ , maximum axial field at injection  $B_{\text{inj}}^{\text{max}}$ , axial field at extraction  $B_{\text{extr}}^w$ , minimum axial field  $B_{\text{cent}}$ , radial field at wall  $B_{\text{hexa}}^w$ , radial field at pole (permanent magnets)  $B_{\text{hexa}}^{\text{pole}}$ , axial distance between walls (from injection to extraction)  $L_{ww}$ , plasma chamber diameter  $\Phi_w$ , frequency  $F$

	Caprice	AECR	Riken	SC-ECR	SERSE
$B_{\text{inj}}^w$ (T)	1.2	1.4	1.4	1.6	~2.4
$B_{\text{inj}}^{\text{max}}$ (T)	1.3	1.7	1.40	1.6	2.7
$B_{\text{extr}}^w$ (T)	1.0	1.1	1.25		~1.4
$B_{\text{cent}}$ (T)	0.40	0.38	0.47	0.18	0.3–0.4
$B_{\text{hexa}}^w$ (T)	1.04	0.85		0.57	1.55
$B_{\text{hexa}}^{\text{pole}}$ (T)	1.2	1.3	1.4		
$L_{ww}$ (mm)	160	280	270	500	420
$\Phi_w$ (mm)	66	76	74	140	130
$F$ (GHz)	14.5	14 + 10	18	6.4	14.5 + 18

amount of perpendicular velocity received by electrons because of the presence of the second frequency would pull them off of the loss region of velocity space (loss cone), so that they can go back along their trajectory and do not impinge on the walls. Actually, experiments reported on the double frequency operation often mention many difficulties to reach a steady state regime with a net performance benefit. With respect to single frequency operation, the double frequency operation would induce an enhanced degassing rate (supposedly from areas of plasma chamber walls not subject to impinging plasma particles in single frequency operation), that could conversely perturb the source functioning and reduce the performance.

### 3.5. Classical ECRIS performances

The magnetic system of the present ECRIS generation, e.g. the magnetic hexapole made of permanent magnets, has often dictated the ECRIS dimensions (plasma chamber diameter), and to some extent the neutral pumping as well. At high charge states, charge exchange is still important enough to limit the ion production. Therefore the neutral pressure control has become an important issue that was not easily improved in these classical ECRIS. Presented here are a few classical representative ECRIS: the Caprice, AECR, and Riken sources. Their main parameters, magnetic fields, and dimensions, are given in Table 2, and a few extracted noble gas ion beam intensities are given in Table 3.

The Caprice concept, a compact source using a strong iron yoke, as initially designed [8], was the first ECRIS to achieve an outstanding compromise for a multicharged ion source, high charge states, high intensities for medium charge states, high stability, reliability, simplicity, modularity, and easy maintenance. It also has a unique original feature, the coaxial coupling of the rf power, that is now used in many sources. The data presented in Table 3 are those obtained when working with a solid aluminum chamber [7].

The AECR source [12], by far the highest performance classical ECRIS, also has a unique original feature: aside from its large chamber diameter, its engineering design differs from others by the radial pumping slots between the hexapole permanent magnets. These slots achieve an efficient in situ pumping in the plasma chamber that likely explain the performance at high charge states usually obtained in double frequency (10/14 GHz) operation. The AECR source presumably has an efficient electron source from its solid aluminum plasma chamber; a biased disc as shown in Fig. 5 is also used.

The Riken source [13,14] has an axial magnetic field flexible enough to tailor the mirror ratio and the magnetic field gradient without reducing the maximum axial field in the plasma chamber. Therefore the Riken source always has the benefit of its full axial magnetic field (1.4 T), whereas most classical ECRIS do not. The beams of highly charged ions shown in Table 3 were obtained while using a biased disc like the AECR source. The Riken source has achieved

Table 3

Representative performances of classical (left-hand side) and superconducting (right-hand side) ECRIS: ion currents are given in  $e\mu\text{A}$ 

Ion	Caprice	AECR	Riken	SC-ECR	SERSE
O <sup>6+</sup>	1130	1150		930	540
O <sup>7+</sup>	180	306		205	208
O <sup>8+</sup>	20	75		18	55
Ar <sup>11+</sup>	200	270	300	200	257
Ar <sup>14+</sup>	15	82	90	36	84
Ar <sup>16+</sup>	1	25	18	2.5	21
Ar <sup>17+</sup>	0.024	2.3			2.6
Ar <sup>18+</sup>		0.1			0.4
Kr <sup>22+</sup>	7	40		29	66
Kr <sup>23+</sup>	6	29		20	56
Kr <sup>25+</sup>	2	19.4		10	35
Kr <sup>27+</sup>					7.8
Kr <sup>28+</sup>	1	2.3		2	
Kr <sup>29+</sup>					1.6
Xe <sup>27+</sup>	22	37.5	60	50	78
Xe <sup>30+</sup>	1	10	12	5	38.5
Xe <sup>34+</sup>				1.2	5.2
Xe <sup>37+</sup>		1			2.6
Xe <sup>38+</sup>					2

impressive performances in metal ion beams by using the MIVOC method (metal ions from volatile compounds [15]).

#### 4. Superconducting ECRIS

Tables 2 and 3 also give the characteristics of a few operating superconducting sources, the superconducting-electron cyclotron resonance (SC-ECR) and SERSE sources. It is clear from these tables, while comparing both kinds of sources, that sources with large plasmas and high magnetic fields definitely achieve better performances, higher charge states, and higher extracted ion currents, according to the arguments developed above in Secs. 2.1. and 2.2. In these larger sources the neutral pressure control is as critical as in classical sources.

However, the construction of superconducting windings for an ECRIS, such as those of SERSE, which are shown in Fig. 8, has to cope with intrinsic difficulties that are not featured by numbers in Table 2. Because of their magnetic configuration ECRIS have crossed magnetic fields; in superconducting ECRIS this specificity combined with the large number of coil turns makes the straight sections of

hexapole coils undergo huge Lorentz forces (tens of tons!). Therefore the hexapole coils have to be drastically tightened. The least conductor displacement (even by  $\leq 0.5 \mu\text{m}$ !) would deliver enough energy in liquid helium at 4.2 °K to increase the conductor temperature and its resistance. This would make the system unstable and cause the corresponding coil to quench. The whole coil system would rapidly follow as well because of mutual inductance.

The SC-ECR source built at MSU [16] was the first superconducting ECRIS to reach significant magnetic fields, and more precisely to work in the so-called high B mode [17], a magnetic configuration with a high axial magnetic field at injection, and correspondingly a large mirror ratio  $R$ , and a large axial field gradient (seen in Fig. 9). The SC-ECR works at 6.4 GHz, and reaches interesting performances, especially at high charge states because of its large dimensions. However, its hexapole cannot overcome the current working conditions (0.57 T on the chamber walls) for the reasons developed above; therefore the SC-ECR cannot work at higher frequencies.

The SERSE source built by a joint venture between CEA/DRFMC-Grenoble and INFN/LNS-Catania now



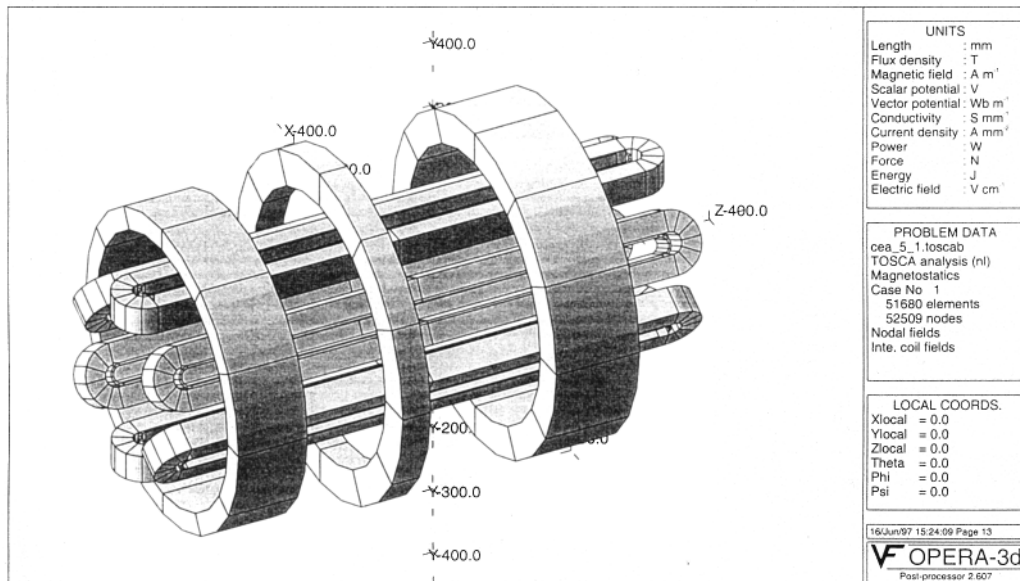


Fig. 8. The configuration of SERSE superconducting coils.

currently works at its design parameters in high B mode [18]. A specific feature of SERSE is shown in Fig. 8. The central coil works with a reverse current that digs the magnetic field for high B-mode operation at 14 GHz. The source permanently uses a biased cylinder as shown in Fig. 5. The data presented in Table 3 were obtained in double frequency 14.5/18 GHz operation. SERSE is the first ECRIS that has all

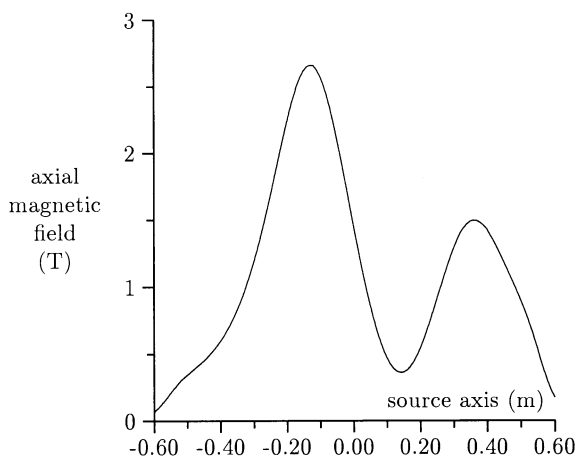


Fig. 9. The high B-mode axial magnetic field of SERSE source.

the desirable features of an ECRIS as developed above: high mirror ratio, high magnetic field, high working rf frequency, and large plasma dimensions. Therefore SERSE correspondingly reaches outstanding performances. Fig. 10 illustrates an unusual ECRIS performance: the SERSE charge state distribution of argon ions with optimized  $\text{Ar}^{16+}/\text{Ar}^{17+}$  ion currents peaks on  $\text{Ar}^{13+}$  ion current, whereas most classical ECRIS peak on  $\text{Ar}^{10+}$  or  $\text{Ar}^{11+}$  at most.

## 5. ECRIS perspectives

Superconducting sources clearly appear as a new ECRIS generation because of their enhanced performances when compared to the best classical ECRIS. Several projects now underway are worth mentioning.

A 28 GHz experiment on SERSE is being carried out by a collaboration between five European laboratories: CERN/Geneva, GSI/darmstadt, INFN-LNS/Catania, IN2P3-ISN/Grenoble, CEA-DRFMC/Grenoble [19]. The objective of this experiment is to achieve high intensity ( $\sim 1$  mA) pulsed currents (a few 100  $\mu\text{s}$ , a few Hz) of  $\text{Pb}^{27+}$  ions! Although

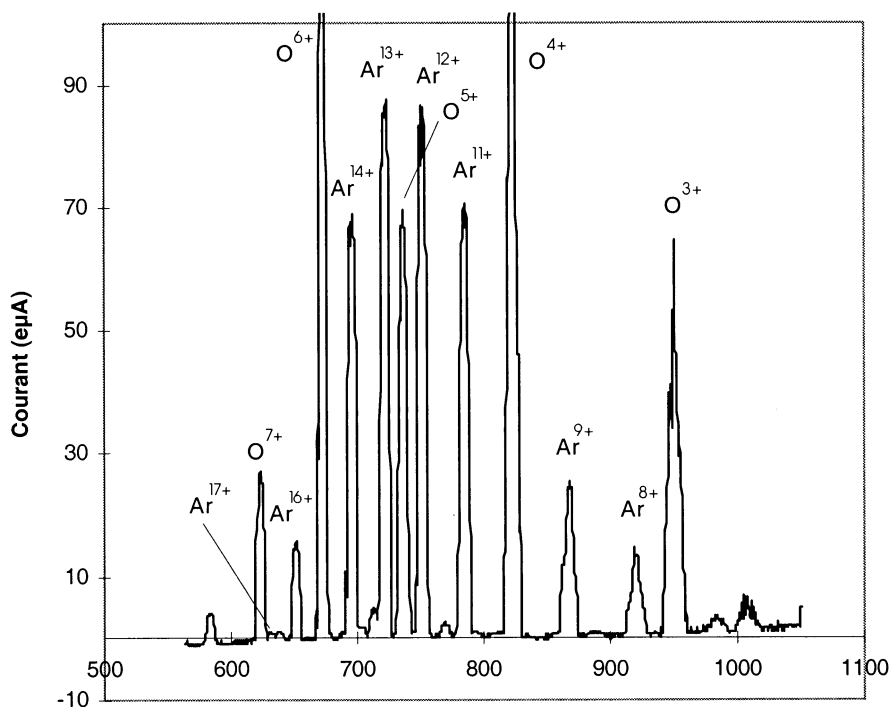


Fig. 10. The SERSE extracted argon ion current distribution when optimizing Ar<sup>16+</sup> current, oxygen 16 as a mixing gas.

SERSE, when working at 28 GHz, has only a mirror ratio as given by formula (2),  $R \sim 1.5$ , the objective of this 28 GHz experiment should be obtained in afterglow mode. This is going to be the first experiment using the gyrotron technology for microwave application to ECRIS.

The so-called “third generation ECR ion source” [20], being constructed at the 88-inch cyclotron in Berkeley, has design characteristics similar to SERSE, although boosted and more demanding ( $B_{inj}^{max} = 4$  T,  $B_{hexa}^w = 2.4$  T,  $\Phi_w = 150$  mm). One of the most important objectives of this facility is to achieve a normal operation at 28 GHz while keeping a mirror ratio,  $R \sim 2$ , like in the best classical ECRIS. The performance should be quite impressive. The concept of multifrequency operation was also mentioned for this project.

The liquid He-free SC-ECRIS [14], which should soon be ready for operation at the Riken Accelerator Research Facility in Japan, is a quite interesting and attractive hybrid concept. The magnetic system

( $B_{inj}^{max} = 3$  T,  $B_{hexa}^w = 1.2$  T,  $\Phi_w = 80$  mm) has a permanent magnet hexapole. A compact refrigerator commercially available is used to cool the solenoid coils. Although the magnetic field of this source is close to that of SERSE, its performance at high charge states should not be as good because of its small plasma chamber diameter. However, the concept of liquid He regeneration cryocooler utilized by this source is an important technological step.

The GYROSERSE project of INFN-LNS/Catania [21] is more ambitious than the Berkeley third generation ECRIS. GYROSERSE, which has not yet been funded, is designed in order to operate in the range 28–35 GHz ( $B_{inj}^{max} = 4.5$  T,  $B_{hexa}^w = 2.7$  T,  $\Phi_w = 190$  mm) in high B mode and correspondingly with  $R > 2$ . Outstanding performances should be achieved.

Aside from the problems of superconducting windings construction mentioned above, this new ECRIS generation should meet with specific drawbacks relating to its high performances. Whereas most classical

sources operate with a total extracted ion current usually lower than 10 electrical mA (emA) with extraction voltages in the range 15–30 kV, superconducting sources working at 28 GHz and higher frequencies are expected to deal with total extracted ion currents of several tens of emA and as large as 100 emA at most. The extraction voltages will likely reach the range 40–60 kV. This makes the design and computation of future extraction systems correspondingly more complex. Other technological issues of this new ECRIS generation refer to the oversized waveguides and rf launching systems to be used with gyrotrons at 28 GHz and higher. The rf power lines from gyrotrons are usually oversized cylindrical waveguides in order to reduce the losses. The behavior of ECRIS with such a rf injection is unknown. At high extraction voltage the use of a normal dc break between rf waveguides and source body becomes difficult, and the rf power transfer system may become a critical issue. Technical solutions to directly couple the rf power to the source by emitting/receiving antennas have to be carefully examined.

Whereas classical ECRIS were essentially based on plasma physics concepts, electron cyclotron resonance heating, and plasma confinement, conversely, the new ECRIS generation is essentially technology dependent. All the above projects of this new ECRIS generation strongly depend upon the development of sophisticated technologies: superconducting technology, gyrotron and high frequency microwave technologies, and high voltage extraction.

## References

- [1] R. Geller, *Electron Cyclotron Resonance Ion Sources and ECR Plasmas*, Institute of Physics, Bristol, 1996, and references therein.
- [2] G. Melin, A. Girard, in *Accelerator-Based Atomic Physics Techniques and Applications*, S.M. Shafroth, J.C. Austin (Eds.), American Institute of Physics, New York, 1997, p. 33; A. Girard, G. Melin, *Nucl. Instrum. Methods Phys. Res. A* 382 (1996) 252.
- [3] A. Girard, C. Perret, C. Lécot, F. Bourg, H. Khodja, G. Melin, *Proceedings of the 1996 International Conference on Plasma Physics*, H. Sugai, T. Hayashi (Eds.), Nagoya, Japan, 1997, Vol. 1, p. 462; A. Girard, C. Perret, G. Melin, C. Lécot, *Rev. Sci. Instrum.* 69 (1998) 1100; C. Perret, A. Girard, H. Khodja, G. Melin, *Phys. Plasmas* 6 (1999) 3408.
- [4] C. Barué, M. Lamoureux, P. Briand, A. Girard, G. Melin, *J. Appl. Phys.* 76 (1994) 2662.
- [5] G. Melin, A.G. Drentje, A. Girard, D. Hitz, *Proceedings of the 14th International Workshop on ECR Ion Sources*, CERN, Geneva, May 1999, p. 13.
- [6] G. Douyset, H. Khodja, J.P. Briand, *Proceedings of the IXth International Conference on the Physics of Highly Charged Ions*, Bensheim, 1998 (unpublished).
- [7] D. Hitz, F. Bourg, M. Delaunay, P. Ludwig, G. Melin, M. Pontonnier, T.K. Nguyen, *Rev. Sci. Instrum.* 67 (1996) 883.
- [8] B. Jacquot, F. Bourg, R. Geller, *Nucl. Instrum. Methods A* 254 (1987) 13; B. Jacquot, M. Pontonnier, *Nucl. Instrum. Methods A* 287 (1990) 341; *ibid.* 295 (1990) 5.
- [9] T. Nakagawa, *Jpn. J. Appl. Phys.* 30 (1991) 930.
- [10] C.E. Hill, K. Langbein, *Rev. Sci. Instrum.* 69 (1998) 643.
- [11] Z.Q. Xie, C.M. Lyneis, *Rev. Sci. Instrum.* 66 (1995) 4218.
- [12] Z.Q. Xie, C.M. Lyneis, *Proceedings of the 13th International Workshop on ECR Ion Sources*, College Station, TX, February 1997, D.P. May, J.E. Ramirez (Eds.), p. 16.
- [13] T. Nakagawa et al., *Proceedings of the 13th International Workshop on ECR Ion Sources*, College Station, TX, February 1997, D.P. May, J.E. Ramirez (Eds.), p. 10.
- [14] T. Nakagawa et al., *Proceedings of the 14th International Workshop on ECR Ion Sources*, CERN, Geneva, May 1999, p. 1.
- [15] H. Koivisto, J. Ärje, M. Nurmia, *Nucl. Instrum. Methods B* 94 (1994) 291.
- [16] T.A. Antaya, *J. Phys. Colloq.* C1 50 (1989) 707.
- [17] T.A. Antaya, S. Gammino, *Rev. Sci. Instrum.* 65 (1994) 1723; T.A. Antaya et al., *Proceedings of the Third International Conference on Radioactive Nuclear Ion Beams*, East Lansing, MI, May 1993.
- [18] G. Ciavola, S. Gammino, P. Briand, G. Melin, P. Seyfert, *Rev. Sci. Instrum.* 65 (1994) 1057; G. Ciavola, S. Gammino, et al., *Rev. Sci. Instrum.* 67 (1996) 889; P. Ludwig et al., G. Ciavola, S. Gammino et al., *Proceedings of the 13th International Workshop on ECR Ion Sources*, College Station, TX, February 1997, D.P. May, J.E. Ramirez (Eds.), p. 119; P. Ludwig et al., G. Ciavola, S. Gammino et al., *Rev. Sci. Instrum.* 69 (1998) 653; P. Ludwig et al., G. Ciavola, S. Gammino et al., *Rev. Sci. Instrum.* 69 (1998) 4082; S. Gammino, G. Ciavola, L. Celona, M. Castro, F. Chines, S. Marletta (unpublished).
- [19] N. Angert et al., *Proceedings of the 14th International Workshop on ECR Ion Sources*, CERN, Geneva, May 1999, p. 220.
- [20] C.M. Lyneis, Z.Q. Xie, *Proceedings of the 12th International Workshop on ECR Ion Sources*, Riken, Japan, April 1995, p. 119; C.M. Lyneis, Z.Q. Xie, C.E. Taylor, *Proceedings of the 13th International Workshop on ECR Ion Sources*, College Station, TX, February 1997, D.P. May, J.E. Ramirez (Eds.), p. 115; M.A. Leitner et al., *Proceedings of the 14th International Workshop on ECR Ion Sources*, CERN, Geneva, May 1999, p. 66.
- [21] S. Gammino, G. Ciavola, L. Celona (unpublished).